Cardiovascular Pathology 41 (2019) 29–37

Contents lists available at ScienceDirect

Cardiovascular Pathology

Original Article

The role of hemodynamics in bicuspid aortopathy: a histopathologic study☆,☆☆,★,★★

Nimrat Grewal [a,b,*], Evaldas Girdauskas [c,d], Marco DeRuiter [b], Marie-Jose Goumans [e], Robert E Poelmann [f], Robert J.M. Klautz [a], Adriana C. Gittenberger-de Groot [b,f]

[a] Department of Cardiothoracic Surgery, Leiden University Medical Center, Leiden, The Netherlands
[b] Department of Anatomy and Embryology, Leiden University Medical Center, Leiden, The Netherlands
[c] Department of Cardiovascular Surgery, University Heart Center Hamburg, Germany
[d] Department of Cardiac Surgery, Central Hospital Bad Berka, Bad Berka, Germany
[e] Department of Molecular Biology, Leiden University Medical Center, Leiden, The Netherlands
[f] Department of Cardiology, Leiden University Medical Center, Leiden, The Netherlands

ARTICLE INFO

Article history:
Received 23 November 2018
Received in revised form 25 March 2019
Accepted 26 March 2019

Keywords:
Bicuspid aortic valve
Tricuspid aortic valve
Hemodynamics
Aortopathy
Histopathology

ABSTRACT

Background: A bicuspid aortic valve (BAV) is the most common congenital cardiac malformation and is associated with ascending aortic dilation in 60%–80% of patients. In this study, we aimed to address the role of hemodynamic influences on the development of aortopathy in BAV patients.
Patient and methods: BAV (n=36) and tricuspid aortic valve (TAV) patients (n=17) undergoing aortic valve replacement underwent preoperative flow magnetic resonance imaging (MRI) assessment to detect the area of maximal flow-induced stress in the proximal aorta. Based on these MRI data, paired ascending aortic wall samples [i.e., area of maximal jet impact (jet sample) and the opposite aortic wall (nonjet sample)] were collected during surgery. To study and describe the effects of jet stream on the complete vascular wall, a pathology score was developed based on the recently published aortic consensus paper statement on surgical pathology of the aorta using routine histologic stainings (resorcin fuchsin, hematoxylin–eosin, and Movat) and immunohistochemistry (alpha smooth muscle actin, smooth muscle 22 alpha, platelet endothelial cell adhesion molecule).
Results: Comparing the jet and nonjet samples in both BAV and TAV, regions of maximal jet impact did not show any difference in the pathology score in the adventitia and the middle and outer media. In the jet samples, the inner media however showed loss of actin expression in both BAV (P<.0001) and the TAV (P=.0074), and the intimal thickness was significantly enlarged in both patient groups (BAV P=.0005, TAV P=.0041), which was not accompanied by loss of elastic lamellae or vascular smooth muscle cell nuclei.
Conclusions: In our study population, we could not demonstrate a potential distinct role for hemodynamics in the development of aortopathy in BAV patients even if corrected for aortic diameter, raphe position, or whether the valve is stenotic or regurgitant. The intimal layer and inner media however showed alterations in all jet specimens.

1. Introduction

Bicuspid aortic valve (BAV) is the most common congenital cardiac malformation with a prevalence of 1%–2% in the general population. Around 60%–80% of BAV patients develop aortic dilation (also called bicuspid aortopathy), which is associated with an increased risk of life-threatening complications [1]. Despite the great disease burden of BAV, to date, the exact pathogenesis of bicuspid aortopathy is not yet sufficiently understood. Studies which have focused on the aortic complications in BAV patients have looked either for genetic causal factors or for the influences of hemodynamics on the ascending aortic wall.

We at least know that the BAV ascending aortic wall is intrinsically different with less differentiated vascular smooth muscle cells

☆ Funding sources: This research did not receive any specific grant from funding agencies in the public, commercial, or not-for-profit sectors.
☆☆ Disclosures: none.
★ Conflict of interest: The authors declare that they have no conflict of interest.
★★ Journal subject terms: basic science research, vascular biology, aneurysm, aortic dissection, vascular disease
* Corresponding author at: Department of Cardiothoracic Surgery, Leiden University Medical Center, Postal zone: K-6-S; P.O. Box 9600, 2300 RC Leiden, The Netherlands. Tel.: +31 52698022; fax: +31 71-526 6809.
E-mail address: n.grewal@lumc.nl (N. Grewal).

https://doi.org/10.1016/j.carpath.2019.03.002

(VSMCs) as compared to the population with a tricuspid aortic valve (TAV) [2–5]. The aorta in BAV is characterized not only by immaturity of the VSMCs of the ascending aorta but also by less aging histopathology features, such as inflammation, apoptosis, and cystic medial degeneration [6]. As not all BAV patients have an increased risk for aortopathy, current studies are aiming at finding predictive markers for aortic complications in BAV [3,7]. In our previous study, we identified a set of markers expressed in the VSMCs of the ascending aorta, associated with vascular remodeling, vascular differentiation, and VSMC relaxation [3]. These findings make it plausible that aortopathy in BAV is associated with pathogenetic processes in the aortic media.

Besides histopathological differences between BAV and TAV, the role of valve related hemodynamics in the development of aortic complications in BAV has also been studied [8–10]. Flow-sensitive cardiac magnetic resonance imaging (CMR) with full volumetric coverage of the ascending aorta (four-dimensional flow CMR) can visualize and measure aortic three-dimensional blood flow patterns, such as flow jets, vortices, and helical flow. It has been shown that nonstenotic or regurgitant BAVs are associated with disturbed flow patterns in the ascending aorta, with regional increases in wall shear stress [11,12].

The question, however, remains whether the impact of jet on the ascending aortic wall is sufficient to explain the observed structural differences of the aortic wall between BAV and TAV. As jet streams hit the endothelial cells and intimal layer initially, it is difficult to understand how that would lead to aortic dilation and dissection which are mainly characterized by pathogenetic features of the aortic media.

In this study, we therefore aimed to study the effects of hemodynamics on the *complete* vascular wall in both TAV and BAV populations, knowing that the jet stream affects the intimal layer primarily but could reflect on the pathologic features in the aortic media. We measured the area of maximal jet impact by flow magnetic resonance imaging (MRI) and analyzed the histopathology characteristics in the intima and media in paired jet and nonjet samples of aortic wall tissue. We further studied whether the hemodynamic effects on the aortic wall can be related to dilation of the ascending aorta, the raphe position in the valve cusps, or stenosis or insufficiency of the aortic valve.

Earlier, we have reported the aortic wall histopathology in jet and nonjet cases [13]. We were, however, unsatisfied by the lack of standardization we could achieve on the histological aspects, which hampers comparison across studies. We have now applied a standardized approach using the recently published aortic consensus paper statement on surgical pathology of the aorta [14] and added a number of parameters based on immunohistochemistry resulting in a well-defined pathology score.

The purpose of this study is to evaluate whether the thus developed pathology score is functional in the description of the ascending aortic wall in BAV patients and analyze a possible correlation between hemodynamics and vessel wall structure in aortopathy in BAV patients as compared to TAV patients.

2. Material and methods

2.1. Study population and preoperative cardiac phase-contrast cine MRI examination

Over a period of 2 years, all consecutive patients with a BAV or a TAV with stenosis or regurgitation undergoing aortic valve replacement (AVR) with or without concomitant proximal aortic replacement were evaluated prospectively at the Central Hospital, Bad Berka, Germany. A total of 36 BAV patients (mean age 55.8±8.7 years, 72% male) and 17 TAV (mean age 60±8.9 years, 82% male) were included in the study.

For this study sample, collection and handling were carried out according to the official guidelines of the Medical Ethical Committee of the Central Hospital Bad Berka. All patients gave written informed consent.

Table 1
Patient characteristics

Characteristic	TAV (n=17)	BAV (n=36)
Age (years)	60±8.9	55.8±8.8
Gender		
Male n (%)	14 (82%)	26 (72%)
Female n (%)	3 (18%)	10 (28%)
Ascending aortic diameter (mm)	45.1±7.2	44.0±8.1
Aortic valve pathology		
Aortic stenosis n=	7	28
Aortic regurgitation n=	10	8
Raphe position		
RCC/LCC n=	NA	28
RCC/NCC n=	NA	8

RCC/LCC: raphe between right coronary cusp and left coronary cusp. RCC/NCC: raphe between right coronary cusp and non-coronary cusp.

In all patients, morphology and function of the aortic valve were assessed preoperatively by echocardiography and cardiac phase-contrast cine MRI. An aortic valve was considered bicuspid if two-dimensional short-axis imaging of the aortic valve demonstrated the existence of only two commissures delimiting two aortic valve cusps. The surgeon however made the final decision regarding the bicuspidy of the aortic valve based on the intraoperative description of valve anatomy, i.e., the existence of three normal commissures for TAV and two normal commissures for BAV. Aortic valve stenosis and regurgitation were defined according to the valvular guidelines [15]. The diameter of the proximal aorta was measured preoperatively by means of transthoracic echocardiography and MRI. Dilation was defined by reaching an ascending aortic wall diameter of 45 mm or more [16]. Patient characteristics are summarized in Table 1.

All patients underwent cardiac phase-contrast cine MRI examination preoperatively to detect the area of maximal jet impact in the proximal ascending aorta. A single noncontrast cardiac MRI (Avanto 1.5-T scanner; Siemens, Erlangen, Germany) which included structural, functional, and phase-velocity-encoded imaging of the left ventricular outflow tract and the proximal aorta was performed as has earlier been described [17]. Fig. 1 shows the location of the jet and the angle at which the flow jet hits the aortic wall in the flow velocity-encoded window.

2.2. Sample processing and routine histology

Based on preoperative MRI analysis, two aortic wall samples were collected from the aortotomy incision in patients who underwent isolated AVR only and from intraoperatively excised aortic tissue in the patients who required simultaneous ascending aortic replacement. The first aortic specimen (the so-called jet sample) was obtained from the area of contact between the systolic transvalvular flow jet and the aortic wall, as determined by preoperative MRI analysis (i.e., the segment of aortic circumference in direct contact with the flow jet). The second sample (i.e., nonjet sample) was collected from the opposite aortic wall. Aortic samples were obtained from the aortotomy incision; the remaining tissue was not used for research purposes. In patients with replacement of the ascending aorta, the samples were approximately 1.0–1.5 cm^2. In cases of an isolated aortic valve surgery, the specimen was approximately 0.3–0.5 cm^2. The height of aortotomy incision was tailored individually in order to correspond with the preoperative MRI data.

Both samples were fixed in 4.5% pH buffered formalin and embedded in paraffin in the Institute of Pathology, University Hospital Jena, Germany. In the Leiden University Medical Center, transverse sections were mounted on precoated Starfrost slides (Klinipath BV, Duiven, the Netherlands).

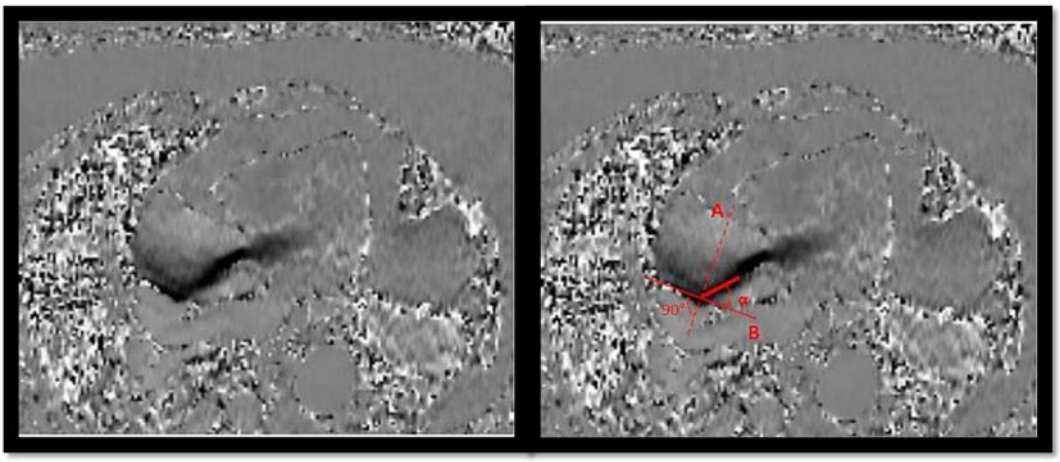

Fig. 1. CMR image. Angle between systolic peak velocity flow jet and the aortic area in direct contact with the flow jet as identified by CMR (flow velocity-encoded phase-contrast imaging). (A) Cross-sectional line across the proximal aorta at the point where the systolic flow jet contacts on the aortic wall; (B) tangential line, perpendicular to line A; $\alpha =$ angle between line B and vector of transvalvular flow (i.e., jet/aorta angle). Figure adapted from Girdauskas et al. [47].

2.3. Histopathologic parameters and analysis

Transverse sections (5 μm) were stained with hematoxylin–eosin (HE), resorcin fuchsin (RF), alpha smooth muscle actin (αSMA), and smooth muscle 22 alpha (SM22α). The staining protocols have been described in detail in a previous paper [2] of our group. Movat pentachrome staining was further performed on 4-μm sections; the staining protocol used was as described before [18]. Immunofluorescence staining was performed with platelet endothelial cell adhesion molecule (PECAM)-1 antibody (M-20, sc-1506) to visualize the endothelial cells.

Sections were studied with a Leica BM500 microscope equipped with plan achromatic objectives (Leica Microsystems, Wetzlar, Germany).

The developed pathology score is based on the recently published aortic consensus paper statement on surgical pathology of the aorta [14] using the routine histologic stainings with HE, RF, and Movat for statement features 1–3 with additional parameters using immunohistochemistry (features 4–7). The features were studied on three predetermined locations (left, middle, and right) of every section, which we refer to as "microscopic fields," maintained in evaluation of all stainings on sister sections. Different from the consensus statement, all features were indexed from 0 (none), 2 (mild), 4 (moderate) to 6 (severe) on the three predetermined locations as we have performed this in a previous study [19]. As the study mainly used surgical biopsy material, we could not evaluate six different sites of the aortic wall as proposed in the consensus pathology statement. The following features were studied:

1. Medial elastic fiber degradation (EFD) indexed from 0 (none), 2 (mild), 4 (moderate) to 6 (severe);

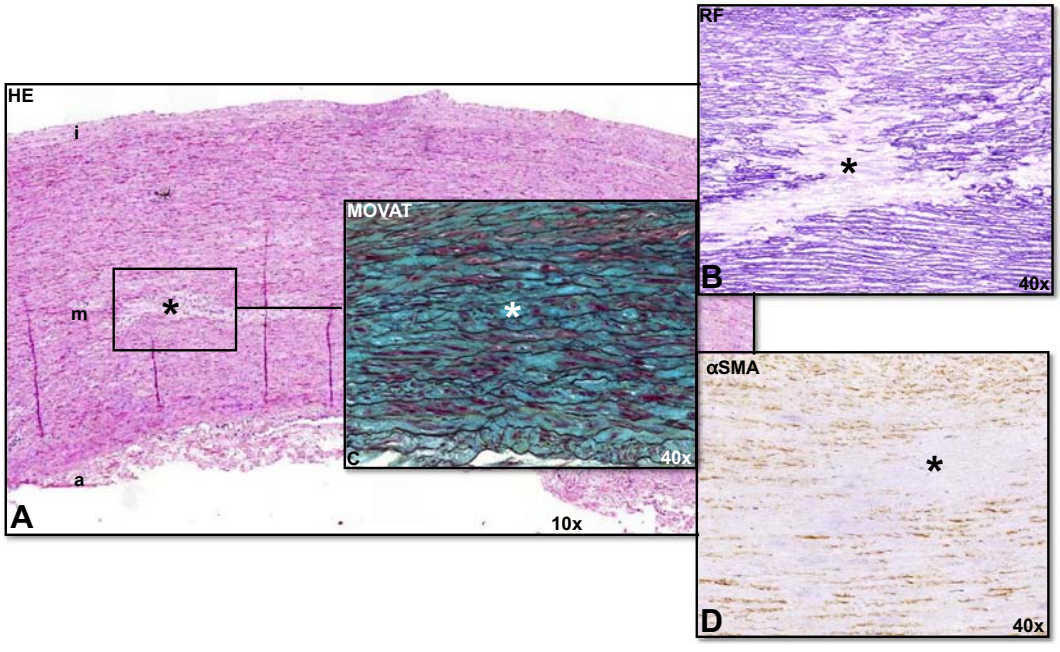

Fig. 2. Histopathologic features. Transverse histologic sections stained with HE (5 μm), RF (5 μm), Movat pentachrome staining (4 μm), and αSMA (5 μm) in the ascending aortic wall in a dilated tricuspid aortic valve. (A) An HE-stained overview of the intima (i), media (m), and adventitia (a), with medial degeneration (asterisk). (B) A detail of the medial layer with EFD (asterisk) in an RF-stained section. (C) A detail of the medial layer with MEMA (asterisk) in a Movat-pentachrome-stained section. (D) A detail of the medial layer with SMCNL (asterisk) in an αSMA-stained section. Magnification: A, 10×; B–D, 40×.

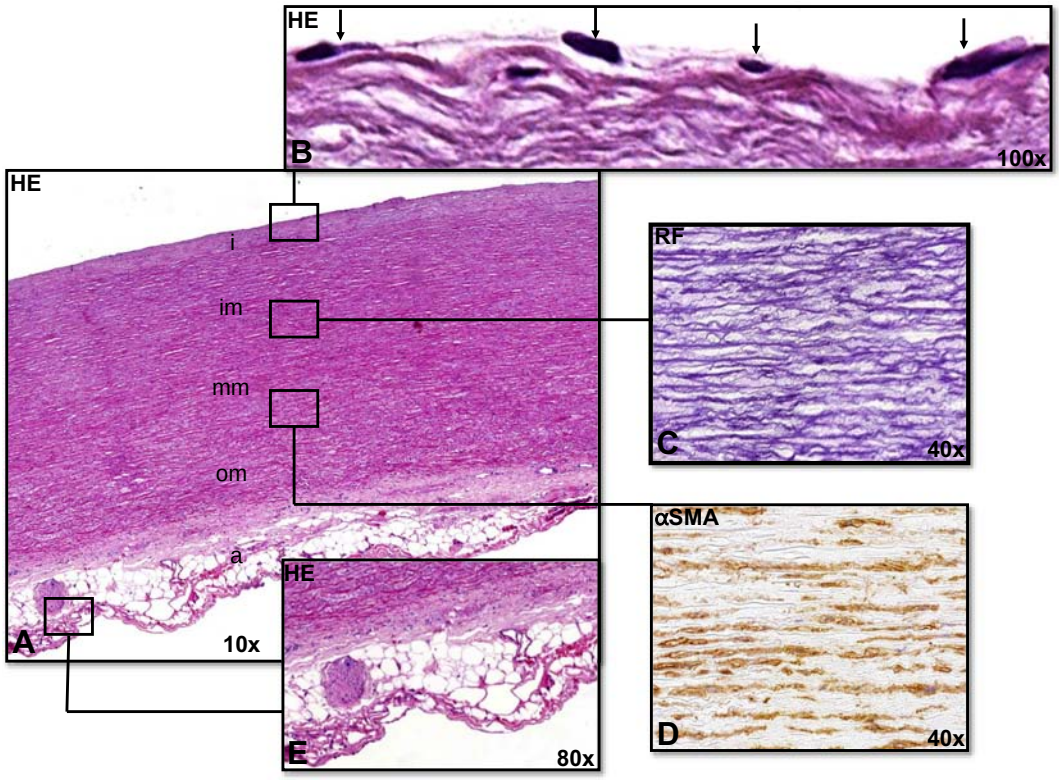

Fig. 3. The normal ascending aortic wall. Transverse histologic sections (5 μm) stained with HE, RF, and αSMA of a nondilated ascending aortic specimen in a tricuspid aortic valve patient. (A) The ascending aortic wall consists of three layers: the intima (i); media, further subdivided into an inner media (im), middle media (mm), and outer media (om); and adventitia (a). (B) The intima consists of an endothelial cell layer (arrows) lining the aortic luminal surface and a subendothelial layer of loosely organized elastic fibers and VSMCs. (C) RF-stained section showing the elastic fibers the media consists of. (D) αSMA-stained section showing the VSMCs in the media. (E) HE-stained section; the adventitia predominantly consists of loose fibrous tissue containing nerve fibers, fibroblasts, adipocytes, and vasa vasorum lined by endothelium and VSMCs. Magnification: A, 10×; B, 100×; C and D, 40×; E, 80×.

2. Medial mucoid extracellular matrix accumulation (MEMA) indexed from 0 (none), 2 (mild), 4 (moderate) to 6 (severe);
3. Smooth muscle cell nuclei loss (SMCNL) indexed from 0 (none), 2 (mild), 4 (moderate) to 6 (severe).

An example of the scored pathologic features EFD (2A, B), MEMA (2A, C), and SMCNL (2A, D) is presented in Fig. 2.

Additional (immuno)histopathological features turned out to be needed to provide a more in-depth insight into the differences between TAV and BAV aortopathy.

1. Medial VSMC differentiation, based on the expression of the differentiated VSMC marker SM22α [20], indexed from 0 (no expression in VSMCs), 2 (expression in less than one third of all VSMCs), 4 (expression in two thirds of all VSMCs) to 6 (expression in more than two thirds of all VSMCs).
2. An extra analysis on the expression of αSMA in the inner media indexed from 0 (expression in less than one third of all VSMCs) to 6 (expression in more than two thirds of all VSMCs).
3. Intimal architecture, including endothelial cell (PECAM) and subendothelial layer structure and the absolute intimal thickness in μm. The intima is defined as the area between the inner surface of the aortic wall, sometimes lined by still present endothelial cells and the well-structured elastic lamellae of the media (excluding atherosclerotic areas).
4. Intimal atherosclerosis indexed from 0 (none), 2 (mild), 4 (moderate) to 6 (severe).

All specimens were evaluated by two independent researchers, who were blinded to the collection site of aortic specimens (i.e., jet sample versus nonjet sample).

2.4. Statistical analysis

Standard definitions were used for patient variables and outcomes. A statistician from the Leiden University Medical Center was consulted for the analysis. Categorical variables are expressed as percentages, and continuous variables are expressed as mean ± SD with range. All analyses were performed with the IBM SPSS 19.0 software (IBM Corp., New York, NY, USA). For the effect of the nonjet vs. jet, we calculated odds ratios between the two conditions. To accommodate the repeated, within-patient (nonjet vs. jet), four-category, ordered outcomes, we used generalized estimating equations to apply repeated-measures ordinal logistic regression to calculate the odds ratios of the nonjet vs. the jet condition adjusting for possible other predictors. An additional analysis was performed to correct for factors such as raphe position for BAV, aortic dilation, and aortic valve dysfunction (i.e., stenosis or regurgitation).

3. Results

3.1. Differences between the nonjet TAV and BAV specimen

Paired aortic wall samples were collected from the jet and nonjet side from all BAV and TAV patients included in this study. From these samples, the nonjet samples were studied first and used to describe the general histopathologic features in the TAV (n=17) and BAV (n=36) without influences of a maximal jet stream. The studied samples consisted of both dilated (TAV n=10, BAV n=14) and nondilated (TAV n=7, BAV n=22) aorta.

The ascending aortic wall consists of three layers: the intima, media, and adventitia (Fig. 3A). The media can further be subdivided in the approximately equally thick inner, middle, and outer media (Fig. 3A). The

intima consists of an endothelial cell layer lining the aortic luminal surface and a subendothelial layer of loosely organized elastic fibers and VSMCs (Fig. 3B). The media contains VSMCs, elastic fibers, collagen, and interposed glycosaminoglycans of the extracellular matrix, which are arranged in lamellar units (Fig. 3C, D). The adventitia predominantly consists of loose fibrous tissue containing nerve fibers, fibroblasts, adipocytes, and vasa vasorum lined by endothelium and VSMCs (Fig. 3E).

Comparing the TAV and BAV specimen, we found that in all (non- and dilated) TAVs, the intima was significantly thicker (P=.004) as compared to all (non- and dilated) BAVs. Intimal atherosclerosis was significantly more prominent in the dilated TAVs as compared to the nondilated TAVs and all BAVs (non- and dilated) (P<.05).

All (non- and dilated) TAVs had significantly more differentiated VSMCs in the media as compared to all (non- and dilated) BAVs (P=.001). EFD, MEMA, and SMCNL were significantly greater in the dilated TAV specimen as compared to the dilated BAV specimen (P=.018, P=.001, and P=.001, respectively).

3.2. Differences between the jet and nonjet ascending aortic wall in the TAV and BAV population

After studying the nonjet samples of the TAV and BAV population, the jet samples were compared to the nonjet side. Even though jet streams hit the endothelial cells and intimal layer primarily, we first studied the aortic medial changes on the jet side as compared to the nonjet side in, as the aortic consensus statement which forms the base of our pathology score focuses on medial pathology. The findings of the paired comparisons of the pathology score between the jet and nonjet sides within the TAV and BAV study population are summarized in Table 2.

In the TAV population, the pathology score features were not different between jet and the nonjet site for intimal atherosclerosis (P=.569), VSMC differentiation (P=.586), EFD (P=.672), MEMA (P=.514), and SMCNL (P=.987). Differences in pathology score features remained nonsignificant between the jet and nonjet side when studied in the different medial layers (inner, middle, and outer) and after correcting for the aortic diameter, the raphe position, and whether the aortic valve was stenotic or regurgitant.

In the BAV population, the pathology score features were also not different between the jet and nonjet side for intimal atherosclerosis (P=.371), VSMC (P=.395), EFD (P=.744), MEMA (P=.453), and SMCNL (P=.051). Differences in pathology score features remained nonsignificant between the jet and nonjet side when studied in the different medial layers (inner, middle, and outer) and after correcting for the aortic diameter, the raphe position, and whether the aortic valve was stenotic or regurgitant.

Table 2
Pathology score

Features	Score	TAV jet *n* (%)	TAV nonjet *n* (%)	*P* value	Odds ratio	95% CI
Atherosclerosis	0	8 (57)	11 (69)	.569	0.828	0.433–1.585
	2	4 (29)	4 (25)			
	4	1 (7)	1 (6)			
	6	1 (7)	0 (0)			
SMC differentiation	0	1 (7)	0 (0)	.586	1.007	0.982–1.034
	2	1 (7)	2 (13)			
	4	5 (33)	6 (40)			
	6	8 (53)	7 (47)			
EFD	0	7 (44)	6 (38)	.672	1.190	0.532–2.660
	2	4 (25)	6 (38)			
	4	4 (25)	3 (19)			
	6	1 (6)	1 (6)			
MEMA	0	1 (8)	1 (7)	.514	0.715	0.262–1.957
	2	5 (39)	8 (53)			
	4	7 (54)	6 (40)			
	6	0 (0)	0 (0)			
SMCNL	0	6 (40)	5 (33)	.987	0.994	0.467–2.113
	2	3 (20)	5 (33)			
	4	4 (27)	3 (20)			
	6	2 (13)	2 (13)			
Features	Score	BAV jet *n* (%)	BAV nonjet *n* (%)	*P* value	Odds ratio	95% CI
Atherosclerosis	0	33 (91)	30 (91)	.371	1.729	0.521–5.733
	2	1 (3)	1 (3)			
	4	1 (3)	2 (6)			
	6	1 (3)	0 (0)			
SMC differentiation	0	3 (9)	0 (0)	.395	1.517	0.581–3.962
	2	28 (80)	29 (85)			
	4	4 (11)	5 (15)			
	6	0 (0)	0 (0)			
EFD	0	31 (86)	29 (88)	.744	0.920	0.558–1.517
	2	4 (11)	3 (9)			
	4	1 (3)	1 (3)			
	6	0 (0)	0 (0)			
MEMA	0	7 (20)	5 (15)	.453	1.246	0.702–2.210
	2	26 (74)	27 (82)			
	4	2 (6)	1 (3)			
	6	0 (0)	0 (0)			
SMCNL	0	29 (81)	32 (94)	.051	0.235	0.059–1.041
	2	7 (19)	2(6)			
	4	0 (0)	0 (0)			
	6	0 (0)	0 (0)			

CI, confidence interval.

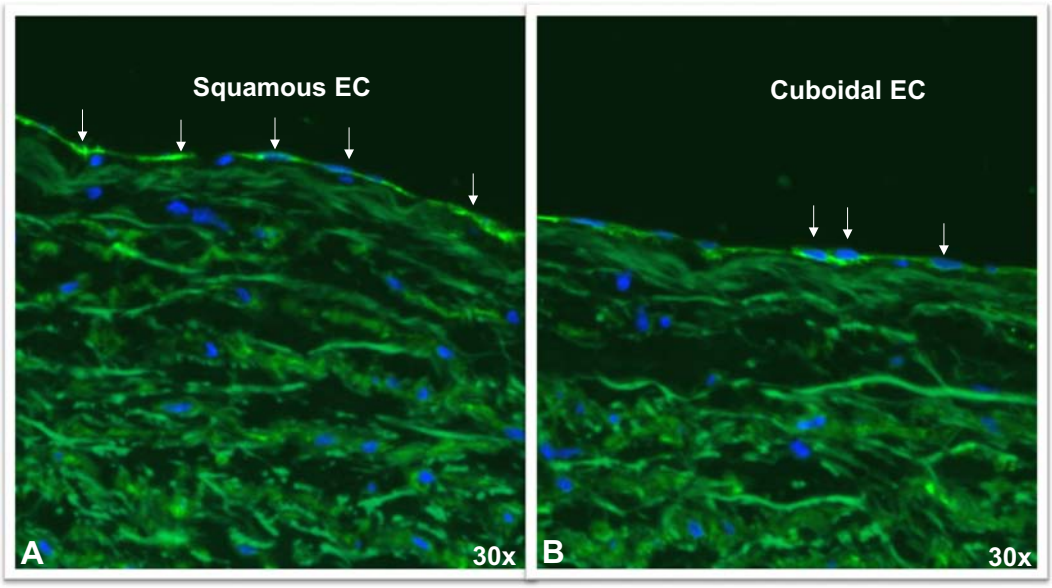

Fig. 4. Transverse histologic sections (5 μm) stained with PECAM of a nondilated ascending aortic specimen in a bicuspid aortic valve patient. (A) Nonjet ascending aortic wall in bicuspid aortic valve, with positive squamous PECAM-stained endothelial cells (indicated with an arrow). (B) Jet ascending aortic wall in bicuspid aortic valve. A change in morphological appearance of part of the endothelial cells is seen from squamous to cuboidal (indicated with an arrow). Magnification: A and B, 30×.

3.3. Additional histopathologic features between the jet and nonjet ascending aortic wall in the TAV and BAV population

Describing the ascending aortic wall in a standardized way using the pathology score thus did not show any significant differences between the jet and nonjet ascending aorta in BAV and TAV, as is indicated above. After studying the intimal layer, we observed a number of additional histopathologic features that were different between the jet and nonjet aorta in both patient groups.

We found that the intima was significantly thicker in all nonjet TAV samples as compared to the nonjet BAV samples. Comparing the jet and nonjet side, we observed a significant increase in intimal thickness on the jet side in both TAV (P=.0041) and BAV (P=.0005) patients. In a subset of the patients in which an intact endothelial layer (PECAM staining for confirmation) was still present and not mechanically torn off (BAV n=17 and TAV n=8), we found morphological differences. In the nonjet specimen, the endothelial cells mostly had a flat elongated morphological appearance. In the jet specimen in both TAV and BAV, the morphological appearance of part of the endothelial cells had changed and showed a cobble shape (Fig. 4 A, B).

Although the number of specimen with intact endothelium was too low for statistical analysis, we observed that the variation in presence of flat elongated and cobble shaped cells was not related to the aortic diameter, the raphe position, or whether the aortic valve was stenotic or regurgitant. As we postulate that the fixation and dilation state of all collected specimen was identical, we did not connect the presence of either elongated or cobble shape morphology to a fixation variety.

In both TAV and BAV, the internal elastic lamella on the borderline with the inner media was more fragmented in the jet specimen as compared to the nonjet specimen. It fanned out, making the borderline between intima and inner media fuzzy. Thus, the distance between the endothelial layer and the first marked internal elastic lamellae appears larger on the jet side in all studied specimen (Fig. 5A–L; graph 5M). Besides an enlargement of the distance between the endothelial layer and the internal elastic lamellae, the structure of the intimal layer was also changed. The intima in the nonjet of all BAV and TAV showed less expression of αSMA (Fig. 5E, K), whereas in the jet samples, there is an obvious increase in expression mostly in the outer intima (Fig. 5F, L) (Table 3). These αSMA-expressing cells were more rounded as compared to the more elongated contractile media VSMCs, thus indicating a possibly synthetic phenotype. In the inner media, as opposed to an increase of αSMA in the outer intima, a significant decrease in αSMA expression was seen on the jet side in both BAV (P<.0001) and TAV (P=.0074) (Fig. 5F, L; graph 5N) (Table 3). The decrease in αSMA expression in the inner media was not accompanied by loss of elastic fibers or loss of nuclei in this area (Fig. 5 compare B, D, F for BAV and H, J, L for TAV).

4. Discussion

A BAV is the most common congenital cardiac malformation, with a population prevalence of 1%–2%. In the BAV population, aortic dissections are eight times more likely as compared to patients with a TAV, and approximately half of the BAV population undergoes cardiac surgery in their lifetime due to aortopathy [1]. As currently used diameter-based aortopathy treatment guidelines are inadequate to predict the increased risk of aortic events in BAV patients, recent studies are focusing on identifying potential aortopathy predicting factors [3,21].

In our earlier studies, we have shown that the ascending aortic wall in BAV patients is characterized by a maturation defect of the VSMCs [2]. But as the lack of differentiation of the aortic wall was seen in all BAV patients, it could not differentiate those patients with an increased risk for aortopathy. In the past few years, several studies have searched for serological and immunohistochemical biomarkers predictive of aortopathy [22–30]. But overall, there was a marked heterogeneity in the biomarker expression patterns reported in the different studies; however, these studies conclude that pathological processes in the aortic media lead to aortic complications in the BAV population.

Besides genetic differences between BAV and TAV patients, growing evidence suggests that the BAV ascending aortic wall is also subject to different hemodynamic influences. The role of hemodynamics on the ascending aortic wall can be studied by MRI and computational fluid dynamics. Several studies have revealed helical blood flow in BAV patients as compared to TAV patients, with eccentric outflow jet patterns disrupting laminar flow and flow impingement zones along the greater curvature of the ascending aorta [31,32]. It is believed that the helical flow is the result of a combination of ventricular twist and torsion during the systole, the fluid mechanics of the aortic valve and root, and the curved geometry of the thoracic aorta [33]. The question however

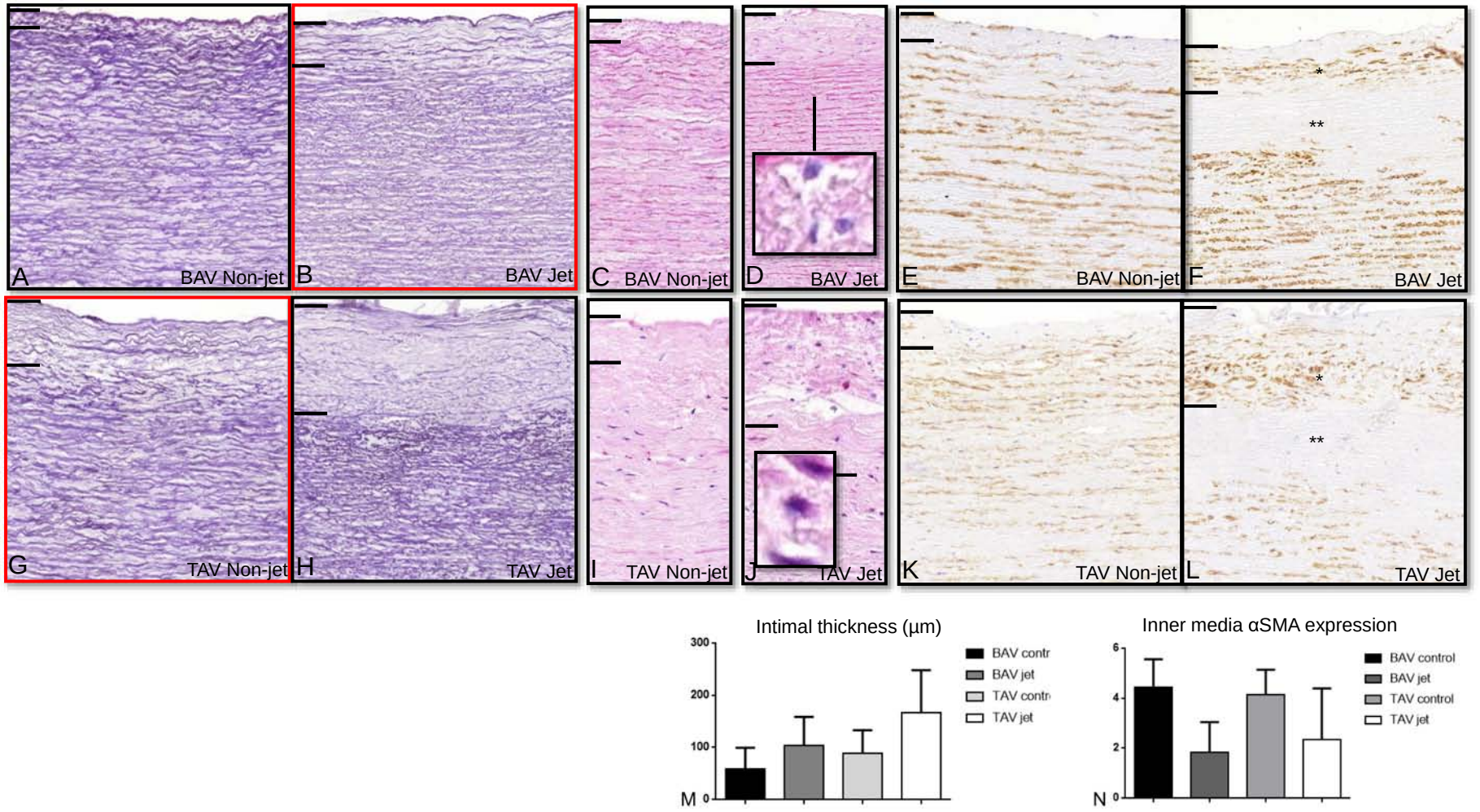

Fig. 5. (A–F) Transverse histologic sections (5 µm) of the ascending aortic wall in the dilated BAVs, stained for RF (A, B), HE (C, D), and αSMA (E, F), comparing the nonjet side (A, C, E) with the jet side (B, D, F). The intimal thickness is indicated between the black lines and is significantly thicker in the jet as compared to the nonjet side. At the jet side, an increase in αSMA expression is seen in the thickened intima (*) and loss of αSMA expression in the inner media (**) (graph M, N), which is however not accompanied by loss of elastic lamellae (B, F) or VSMC nuclei (D, F). (G–L) Transverse histologic sections (5 µm) of the ascending aortic wall in the dilated TAVs, stained for RF (G, H), HE (I, J) and αSMA (K, L), comparing the nonjet side (G, I, K) with the jet side (H, J, L). The intimal thickness is indicated between the black lines and is significantly thicker in the jet as compared to the nonjet side. At the jet side, an increase in αSMA is seen in the thickened intima (*) and loss of αSMA in the inner media (**) (graph M, N), which is however not accompanied by loss of elastic lamellae (H, L) or VSMC nuclei (J, L). The RF-stained sections B and E show that the BAV intima shows similarities with the nonjet TAV after being effected by the jet stream. Magnification: A–L 40×; inserts in D and J, 80×.

Table 3
αSMA expression in BAV and TAV

Patient group Characteristic	TAV nonjet (n=17)	TAV jet (n=17)	BAV nonjet (n=36)	BAV jet (n=36)
Expression in inner media				
0	0	6	0	10
2	1	6	4	21
4	12	3	22	5
6	4	2	10	0
Expression in intima				
0	4	1	9	0
2	8	1	23	3
4	4	11	4	22
6	1	4	0	11

remains whether the observed differences in hemodynamics in BAV and TAV, which initially affect the intimal layer, can explain the increased risk for aortopathy in the BAV population, which seems to be an aortic media problem.

Therefore, in this study, we aimed to correlate the maximal jet impact on the ascending aortic wall to histopathological features in the BAV and TAV population observed in the complete vascular wall.

Describing vascular pathology is complex, and most studies lack a standardization in the methods and description of the vessel wall. Moreover, obtaining a wide range of tissue biopsies of the aorta during surgery is nearly impossible. The lack of standardization and the sampling limitation therefore make it important to have a standard way of analyzing and describing the aorta which would aid in understanding the complex pathogenesis of aortopathy in BAV. In this study, we therefore aimed to describe the aorta in BAV and TAV in a standardized way using a pathology score based on the grading system described in the recently published Cardiovascular Pathology/Association for European Cardiovascular Pathology consensus paper statement on surgical pathology of the aorta [14] with addition of a number of immunohistochemical-based features.

By comparing the nonjet specimen, as identified by MRI, we could confirm differences of our pathology score features between the BAV and TAV which we have earlier described in other patient populations [2,3,34]. When comparing the pathology score features between the jet and nonjet in the BAV and TAV population, we did not observe any difference between both sides.

Recent literature has particularly focused on the hemodynamic influences for the different raphe positions in the BAV population. Mahadevia et al. and Raghav et al. have shown that the normalized flow displacement is a reliable quantification of flow eccentricity as compared to systolic flow angle [35,36]. In their studies, flow displacement was found to be greater in BAV as compared to TAV patients matched for aortic diameter and valvular function [35,36]. They observed a correlation of the distal ascending aorta diameter in BAV patients with fusion of the right and noncoronary cusps (RN-BAV) but not in BAV patients with fusion of the right and left coronary cusps (RL-BAV) [36,37]. Flow displacement has also been identified as a potential marker for BAV aortopathy phenotype, showing that both type 1 aortopathy (involvement of the aortic root) and type 3 (the distal ascending aorta) aortopathy are more common in RN-BAV, whereas type 2 aortopathy (the midascending aorta) is more common in RL-BAV [35,38,39]. Recent data on development of BAV in mouse mutant models show that, for the RN-BAV, there is an absence of development of the noncoronary cusp. This is either by nonseparation of the septal endocardial cushion in the future aortic orifice as seen in the eNOS mutant mouse [40] or by absence of the development of this valve cusp [41]. Neural crest cells and second heart field cells have a distinct contribution to the ascending aorta as well as to the aortic root and semilunar valves and commissures. The balance between the contribution of neural crest cells and second heart field cells is disturbed in both above described models. For the RL-BAV, which in human is the most common raphe position, a proper developmental explanation is still lacking.

On the basis of these literature findings, we also took the aortic diameter, the raphe position, and whether the valve was stenotic or regurgitant into account in the present study;, however, we found that even after correcting for the aortic diameter, the raphe position, and whether the valve was stenotic or regurgitant, there were no differences in the pathology score features between the jet and nonjet in the BAV and TAV population.

After studying the medial layer, we focused on the effects of jet stream on the intimal layer.

In our study population, all TAV patients had a significantly thicker intimal layer as compared to all BAV patients. On the jet side of both patient groups, a significant increase in intimal thickness is seen as compared to the paired nonjet samples, probably as a result of the jet stream. An obvious increase in αSMA-positive VSMC is seen in the outer intima, whereas the inner media shows a significant decrease in expression of αSMA of the VSMCs. In our previous work, we observed loss of αSMA in the middle media in TAV patients with a dilated aorta [2]. The loss of αSMA was in those cases accompanied by loss of elastic fibers and loss of VSMC nuclei in the middle media, characteristic for the pathologic feature cytolytic necrosis (in the consensus statement paper referred to as medial degeneration) and part of cardiovascular aging processes. In this study, the observed loss of αSMA in the inner media in the jet samples of BAV and TAV patients is not accompanied by loss of elastic fibers or loss of VSMC nuclei as can be seen in Fig. 5. Therefore, this observed phenomenon of loss of αSMA is different from the pathologic feature of medial degeneration It is however not clear what causes the difference of αSMA in the jet samples. A possible explanation for the difference in expression on the jet side could be due to migration of VSMCs from the inner media to the outer intima.

We further observed a trend in which more cobble-shaped endothelial cells lined the aorta in the jet specimen as compared to the elongated flat endothelial cells that were observed in the nonjet specimen of all BAV and TAV patients. Endothelial cells do show a heterogenic morphology across vascular beds [42–44]. We postulate that the observed increase in cobble morphology might be related to the development of intimal thickening [45] in the jet specimen.

This study was not designed to explore endothelial to mesenchymal transition [46]; therefore, more research is needed focusing on the possibility of an endothelial transition aspect in BAV and TAV specimen.

In conclusion, we aimed to address the role of hemodynamic influences on the development of aortopathy in BAV patients. In our study population, we could not demonstrate a potential role of hemodynamics in the development of aortopathy leading to dilation in BAV patients even if corrected for aortic diameter, raphe position, or whether the valve is stenotic or regurgitant.

Acknowledgments

None.

References

[1] Michelena HI, Khanna AD, Mahoney D, Margaryan E, Topilsky Y, Suri RM, et al. Incidence of aortic complications in patients with bicuspid aortic valves. JAMA 2011; 306:1104–12.
[2] Grewal N, Gittenberger-de Groot AC, Poelmann RE, Klautz RJ, Lindeman JH, Goumans MJ, et al. Ascending aorta dilation in association with bicuspid aortic valve: a maturation defect of the aortic wall. J Thorac Cardiovasc Surg 2014;148:1583–90.
[3] Grewal N, Gittenberger-de Groot AC, DeRuiter MC, Klautz RJ, Poelmann RE, Duim S, et al. Bicuspid aortic valve: phosphorylation of c-Kit and downstream targets are prognostic for future aortopathy. Eur J Cardiothorac Surg 2014;46:831–9.
[4] Fedak PW, de Sa MP, Verma S, Nili N, Kazemian P, Butany J, et al. Vascular matrix remodeling in patients with bicuspid aortic valve malformations: implications for aortic dilatation. J Thorac Cardiovasc Surg 2003;126:797–806.
[5] Pasta S, Phillippi JA, Gleason TG, Vorp DA. Effect of aneurysm on the mechanical dissection properties of the human ascending thoracic aorta. J Thorac Cardiovasc Surg 2012;143:460–7.
[6] Matthias Bechtel JF, Noack F, Sayk F, Erasmi AW, Bartels C, Sievers HH. Histopathological grading of ascending aortic aneurysm: comparison of patients with bicuspid versus tricuspid aortic valve. J Heart Valve Dis 2003;12:54–9 [discussion 9-61].

[7] Girdauskas E, Petersen J. Update on bicuspid aortic valve aortopathy. Curr Opin Cardiol 2017;32:651–4.
[8] Girdauskas E, Borger MA, Secknus MA, Girdauskas G, Kuntze T. Is aortopathy in bicuspid aortic valve disease a congenital defect or a result of abnormal hemodynamics? A critical reappraisal of a one-sided argument. Eu J Cardiothorac Surg 2011;39:809–14.
[9] Cotrufo M, Della Corte A. The association of bicuspid aortic valve disease with asymmetric dilatation of the tubular ascending aorta: identification of a definite syndrome. J Cardiovasc Med (Hagerstown) 2009;10:291–7.
[10] Hope MD, Hope TA, Meadows AK, Ordovas KG, Urbania TH, Alley MT, et al. Bicuspid aortic valve: four-dimensional MR evaluation of ascending aortic systolic flow patterns. Radiology 2010;255:53–61.
[11] Barker AJ, Markl M, Burk J, Lorenz R, Bock J, Bauer S, et al. Bicuspid aortic valve is associated with altered wall shear stress in the ascending aorta. Circ Cardiovasc Imaging 2012;5:457–66.
[12] Guzzardi DG, Barker AJ, van Ooij P, Malaisrie SC, Puthumana JJ, Belke DD, et al. Valve-related hemodynamics mediate human bicuspid aortopathy: insights from wall shear stress mapping. J Am Coll Cardiol 2015;66:892–900.
[13] Grewal N, Girdauskas E, de Ruiter M, Goumans MJ, Lindeman JH, Disha K, et al. The effects of hemodynamics on the inner layers of the aortic wall in patients with a bicuspid aortic valve. Integr Mol Med 2017;4(5).
[14] Halushka MK, Angelini A, Bartoloni G, Basso C, Batoroeva L, Bruneval P, et al. Consensus statement on surgical pathology of the aorta from the Society for Cardiovascular Pathology and the Association for European Cardiovascular Pathology: II. Noninflammatory degenerative diseases — nomenclature and diagnostic criteria. Cardiovasc Pathol 2016;25:247–57.
[15] Baumgartner H, Hung J, Bermejo J, Chambers JB, Evangelista A, Griffin BP, et al. Echocardiographic assessment of valve stenosis: EAE/ASE recommendations for clinical practice. Eur J Echocardiogr 2009;10:1–25.
[16] Hiratzka LF, Creager MA, Isselbacher EM, Svensson LG, Nishimura RA, Bonow RO, et al. Surgery for aortic dilatation in patients with bicuspid aortic valves: a statement of clarification from the American College of Cardiology/American Heart Association Task Force on Clinical Practice Guidelines. J Am Coll Cardiol 2016;67:724–31.
[17] Girdauskas E, Rouman M, Disha K, Scholle T, Fey B, Theis B, et al. Correlation between systolic transvalvular flow and proximal aortic wall changes in bicuspid aortic valve stenosis. Eur J Cardiothorac Surg 2014;46:234–9 [discussion 9].
[18] van Dijk RA, Virmani R, von der Thusen JH, Schaapherder AF, Lindeman JH. The natural history of aortic atherosclerosis: a systematic histopathological evaluation of the peri-renal region. Atherosclerosis 2010;210:100–6.
[19] Grewal N, Gittenberger-de Groot AC. Pathogenesis of aortic wall complications in Marfan syndrome. Cardiovasc Pathol 2018;33:62–9.
[20] Owens GK, Kumar MS, Wamhoff BR. Molecular regulation of vascular smooth muscle cell differentiation in development and disease. Physiol Rev 2004;84:767–801.
[21] Della Corte A, Bancone C, Quarto C, Dialetto G, Covino FE, Scardone M, et al. Predictors of ascending aortic dilatation with bicuspid aortic valve: a wide spectrum of disease expression. Eur J Cardiothorac Surg 2007;31:397–404 [discussion −5].
[22] Ikonomidis JS, Ivey CR, Wheeler JB, Akerman AW, Rice A, Patel RK, et al. Plasma biomarkers for distinguishing etiologic subtypes of thoracic aortic aneurysm disease. J Thorac Cardiovasc Surg 2013;145:1326–33.
[23] Black KM, Masuzawa A, Hagberg RC, Khabbaz KR, Trovato ME, Rettagliati VM, et al. Preliminary biomarkers for identification of human ascending thoracic aortic aneurysm. J Am Heart Assoc 2013;2:e000138.
[24] Wang Y, Wu B, Dong L, Wang C, Wang X, Shu X. Circulating matrix metalloproteinase patterns in association with aortic dilatation in bicuspid aortic valve patients with isolated severe aortic stenosis. Heart Vessels 2016;31:189–97.
[25] Drapisz S, Goralczyk T, Jamka-Miszalski T, Olszowska M, Undas A. Nonstenotic bicuspid aortic valve is associated with elevated plasma asymmetric dimethylarginine. J Cardiovasc Med (Hagerstown) 2013;14:446–52.
[26] Tzemos N, Lyseggen E, Silversides C, Jamorski M, Tong JH, Harvey P, et al. Endothelial function, carotid-femoral stiffness, and plasma matrix metalloproteinase-2 in men with bicuspid aortic valve and dilated aorta. J Am Coll Cardiol 2010;55:660–8.
[27] Suzuki T, Bossone E, Sawaki D, Janosi RA, Erbel R, Eagle K, et al. Biomarkers of aortic diseases. Am Heart J 2013;165:15–25.
[28] Wu J, Song HF, Li SH, Guo J, Tsang K, Tumiati L, et al. Progressive aortic dilation is regulated by miR-17-associated miRNAs. J Am Coll Cardiol 2016;67:2965–77.
[29] Naito S, Hillebrand M, Bernhardt AMJ, Jagodzinski A, Conradi L, Detter C, et al. The value of circulating biomarkers in bicuspid aortic valve-associated aortopathy. Thorac Cardiovasc Surg 2018;66:278–86.
[30] Schmoker JD, McPartland KJ, Fellinger EK, Boyum J, Trombley L, Ittleman FP, et al. Matrix metalloproteinase and tissue inhibitor expression in atherosclerotic and nonatherosclerotic thoracic aortic aneurysms. J Thorac Cardiovasc Surg 2007;133:155–61.
[31] Mahadevia R, Barker AJ, Schnell S, Entezari P, Kansal P, Fedak PW, et al. Bicuspid aortic cusp fusion morphology alters aortic three-dimensional outflow patterns, wall shear stress, and expression of aortopathy. Circulation 2014;129:673–82.
[32] Kimura N, Nakamura M, Komiya K, Nishi S, Yamaguchi A, Tanaka O, et al. Patient-specific assessment of hemodynamics by computational fluid dynamics in patients with bicuspid aortopathy. J Thorac Cardiovasc Surg 2017;153:S52–62 [e3].
[33] Farthing S, Peronneau P. Flow in the thoracic aorta. Cardiovasc Res 1979;13:607–20.
[34] Grewal N, Franken R, Mulder BJ, Goumans MJ, Lindeman JH, Jongbloed MR, et al. Histopathology of aortic complications in bicuspid aortic valve versus Marfan syndrome: relevance for therapy? Heart Vessels 2015;31(5):795–806.
[35] Mahadevia R, Barker AJ, Schnell S, Entezari P, Kansal P, Fedak PW, et al. Response to letter regarding article, "bicuspid aortic cusp fusion morphology alters aortic three-dimensional outflow patterns, wall shear stress, and expression of aortopathy". Circulation 2014;130:e171.
[36] Raghav V, Barker AJ, Mangiameli D, Mirabella L, Markl M, Yoganathan AP. Valve mediated hemodynamics and their association with distal ascending aortic diameter in bicuspid aortic valve subjects. J Magn Reson Imaging 2018;47:246–54.
[37] Youssefi P, Gomez A, He T, Anderson L, Bunce N, Sharma R, et al. Patient-specific computational fluid dynamics-assessment of aortic hemodynamics in a spectrum of aortic valve pathologies. J Thorac Cardiovasc Surg 2017;153:8–20 [e3].
[38] Della Corte A, Bancone C, Conti CA, Votta E, Redaelli A, Del Viscovo L, et al. Restricted cusp motion in right-left type of bicuspid aortic valves: a new risk marker for aortopathy. J Thorac Cardiovasc Surg 2012;144:360–9 [9.e1].
[39] Della Corte A, Bancone C, Dialetto G, Covino FE, Manduca S, D'Oria V, et al. Towards an individualized approach to bicuspid aortopathy: different valve types have unique determinants of aortic dilatation. Eur J Cardiothorac Surg 2014;45:e118–24 [discussion e24].
[40] Peterson JC, Chughtai M, Wisse LJ, Gittenberger-de Groot AC, Feng Q, Goumans MTH, et al. Bicuspid aortic valve formation: Nos3 mutation leads to abnormal lineage patterning of neural crest cells and the second heart field. Dis Model Mech 2018;11.
[41] Eley L, Alqahtani AM, MacGrogan D, Richardson RV, Murphy L, Salguero-Jimenez A, et al. A novel source of arterial valve cells linked to bicuspid aortic valve without raphe in mice. Elife 2018;7.
[42] Aird WC. Phenotypic heterogeneity of the endothelium: I. Structure, function, and mechanisms. Circ Res 2007;100:158–73.
[43] Reidy MA, Langille BL. The effect of local blood flow patterns on endothelial cell morphology. Exp Mol Pathol 1980;32:276–89.
[44] Levesque MJ, Liepsch D, Moravec S, Nerem RM. Correlation of endothelial cell shape and wall shear stress in a stenosed dog aorta. Arteriosclerosis 1986;6:220–9.
[45] De Reeder EG, Girard N, Poelmann RE, Van Munsteren JC, Patterson DF, Gittenberger-De Groot AC. Hyaluronic acid accumulation and endothelial cell detachment in intimal thickening of the vessel wall. The normal and genetically defective ductus arteriosus. Am J Pathol 1988;132:574–85.
[46] Wesseling M, Sakkers TR, de Jager SCA, Pasterkamp G, Goumans MJ. The morphological and molecular mechanisms of epithelial/endothelial-to-mesenchymal transition and its involvement in atherosclerosis. Vascul Pharmacol 2018;106:1–8.
[47] Girdauskas E, Rouman M, Disha K, Fey B, Dubslaff G, Theis B, et al. Functional aortic root parameters and expression of aortopathy in bicuspid versus tricuspid aortic valve stenosis. J Am Coll Cardiol 2016;67:1786–96.